Process oriented modeling of Lake Ontario hydrodynamics

Leon Boegman
Department of Civil Engineering, Queen's University, Kingston, ON, Canada

Yerubandi R. Rao
National Water Research Institute, Environment Canada, Burlington, ON Canada

ABSTRACT: A three-dimensional hydrostatic Reynolds averaged Navier Stokes equation model has been applied to simulate the ice-free hydrodynamics of Lake Ontario during 2006. The model is compared to field observations to assess its ability to reproduce the fundamental physical processes driving hydrodynamics. The model correctly simulates the seasonal stratification, surface seiches and internal Poincaré waves without adjustment. Scaling of inflows is required to reproduce water levels. Surface topographic and internal waves are simulated; however, these motions are under-resolved with the 2 km horizontal grid used in this study.

1 INTRODUCTION

Coupled hydrodynamic and biogeochemical models are valuable engineering tools for diagnostic and prognostic management studies of lake and reservoir water quality. These models have evolved to the state where they can routinely simulate basin-scale hydrodynamics using 'coarse' horizontal grid resolutions.

For small and medium sized lakes with a characteristic lengthscale (L) less than or equal to the Rossby radius (R), respectively, hydrostatic Reynolds averaged Navier-Stokes equation (RANSE) models have been shown to be capable of resolving the fundamental processes at the basin-scale, including surface seiches and internal Kelvin and Poincaré waves (e.g. Hodges, et al. 2000). However, for large lakes (e.g. the Great Lakes), where $L >> R$, these models are typically calibrated in a qualitative or quantitative manner against temperature and current observations (e.g. León et al. 2005; Schwab & Bedford 1994; Boegman et al. 2001; Prakash et al. 2007). The ability of these models to simulate the fundamental processes in large lakes has not been investigated.

The objective of this study is to apply a hydrodynamic model to Lake Ontario, test the ability of the model to reproduce fundamental basin-scale processes (surface seiche and internal Kelvin and Poincaré waves) and determine the spatial-dynamic structure of these modes.

We thank Jörg Imberger at the Centre for Water Research for providing the ELCOM code and Luis León for helping with its application to L. Ontario. Erin Hall performed the initial model setups. We thank Bob Rowsell for the data collection. This project was funded by Environment Canada and the Ontario Ministry of Environment.

2 METHODS

We apply the three-dimensional estuary and lake computer model (ELCOM) to Lake Ontario during 11 April to 26 October, 2006. ELCOM solves the unsteady RANSE on a 2 km x 2 km horizontal z-level grid. Vertical grid spacing varies from 1 m near the surface to 16 m near the bed. A one-dimensional mixed-layer model is used for turbulence closure of vertical Reynolds stress terms (Hodges et al. 2000). The model is forced with 10-min meteorological data (wind

speed and direction, relative humidity, air temperature and long and short wave solar radiation) recorded by NWRI Environment Canada at stations 1263, 586 and 403 (Fig. 1).

Flow boundary conditions are specified for the Welland Canal, Niagara River, St. Lawrence River at Cornwall (source: Environment Canada), over-lake precipitation and modelled streamflow data (source: NOAA). Evaporation is computed internally in ELCOM.

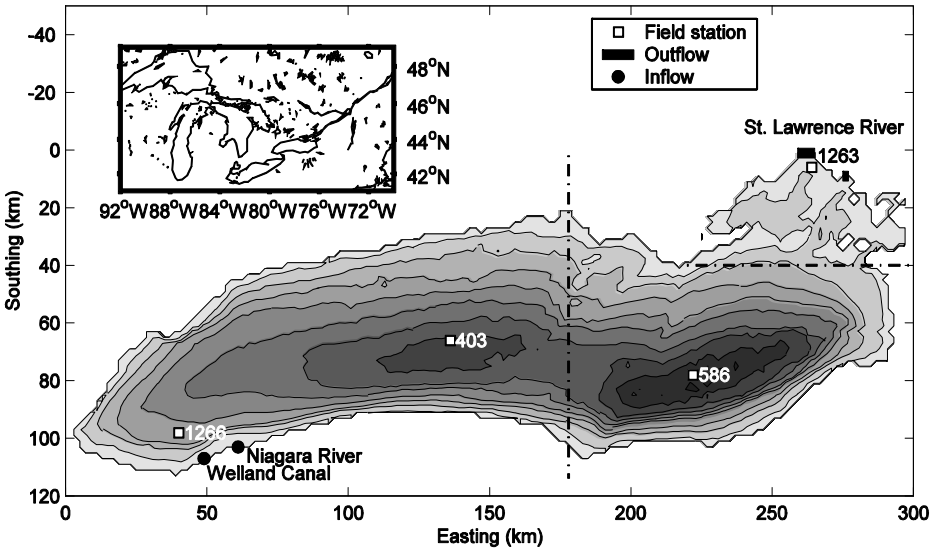

Figure 1. Bathymetric map of Lake Ontario showing the locations of the field stations, inflows and outflows. Distinct meteorological data was applied in each of the three regions delineated by the dash-dot lines as recorded at stations 1263, 586 and 403. The depth contour isobaths interval is 25 m.

3 RESULTS AND DISCUSSION

3.1 *Water levels*

The modelled water levels at stations 1266 and 1263 were compared to nearby water level observations from gauges. The seasonal trends were well modelled when the streamflow data was increased by 20%. Figure 2 shows an example of modeled and observed water levels at the Kingston gauge, where the model result has a 1 d phase shift ahead of the gauge. This could be a manifestation of the spatial distribution of the wind forcing and requires further investigation. The need for increased streamflow is a function of inaccuracies in flow data (e.g. modeled streamflow data) and that ELCOM is not designed to conserve mass during long simulations. The latter effect likely dominates as other models (e.g. CE-QUAL-W2) have been shown to accurately reproduce water levels in the Great Lakes using similar flow data (Boegman et al. 2001).

Spectral energy plots of the water levels (Fig. 3a) show statistically significant peaks in the model result and field data at 12-hrs and at the periods of the first (5.06 hr) and third (2.32 hr) longitudinal surface seiche modes (Hamblin 1982); the 12-hr peak likely being the result of diurnal forcing. There is no energy associated with the ~10 day storm cycle, as seen in Lake Erie (Hamblin 1987; Boegman et al. 2001).

At much lower energy levels, significant peaks corresponding to the first (45 min) and second (22.5 min) transverse surface seiche modes (Denison 1908) are found in the modelled Kingston spectra. These are not evident in the model output at station 1266 and so are likely associated with a north-south barotropic oscillation in the Kingston basin, rather than a true open lake transverse seiche. Due to the hourly sampling interval, this signal is not resolved by the observed gauge data.

3.2 *Temperatures*

Modelled temperature profiles were compared to observed temperatures at stations 403, 586 and 1266. Observed temperatures were recorded every 10 min using HOBO Tidbit loggers at depth

intervals ranging from 0.5 m to 10 m through the water column (source: Environment Canada). The evolution of the temperature profile is well modelled (e.g. Fig. 4a,b), including the formation of a seasonal thermocline at a depth of ~ 15 m, surface layer mixing events (near days 180 and 200) and large and small scale oscillatory motions associated with baroclinic (internal) waves. These results are in general agreement with other model applications to large Canadian lakes (e.g. León et al. 2005; Schwab & Bedford 1994; Boegman et al. 2001). Higher-frequency Poincaré wave oscillations are evident in the observations and model results along the thermocline (Fig. 4c,d). The dominant spectral peak in both the modelled and field data at station 1266 has a period of 16.38 hrs and is identified as an internal Poincaré mode, just below the inertial frequency, f =17.35 hrs (Fig. 3b). A secondary peak, near one half the inertial period, 8.54 hrs, is modeled (statistically significant), but not observed. This peak has been observed by

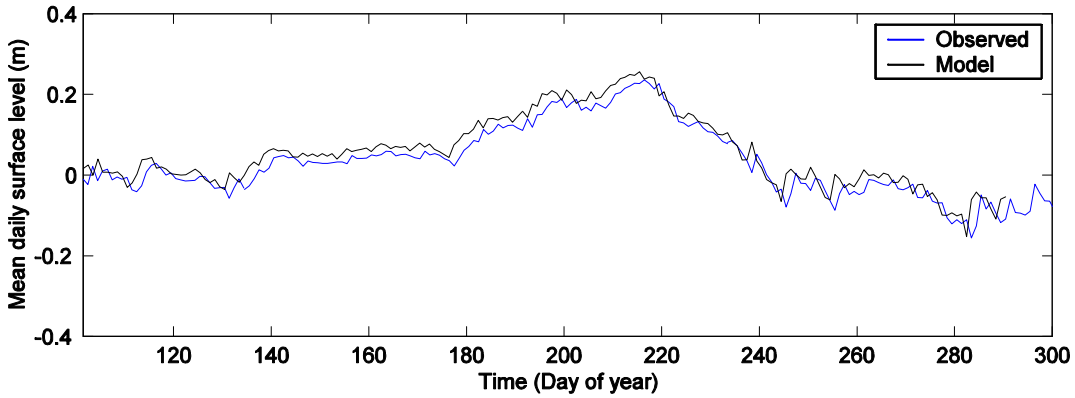

Figure 2: Comparison of mean daily water level deviation observed at the Kingston gauge station and modelled at station 1263.

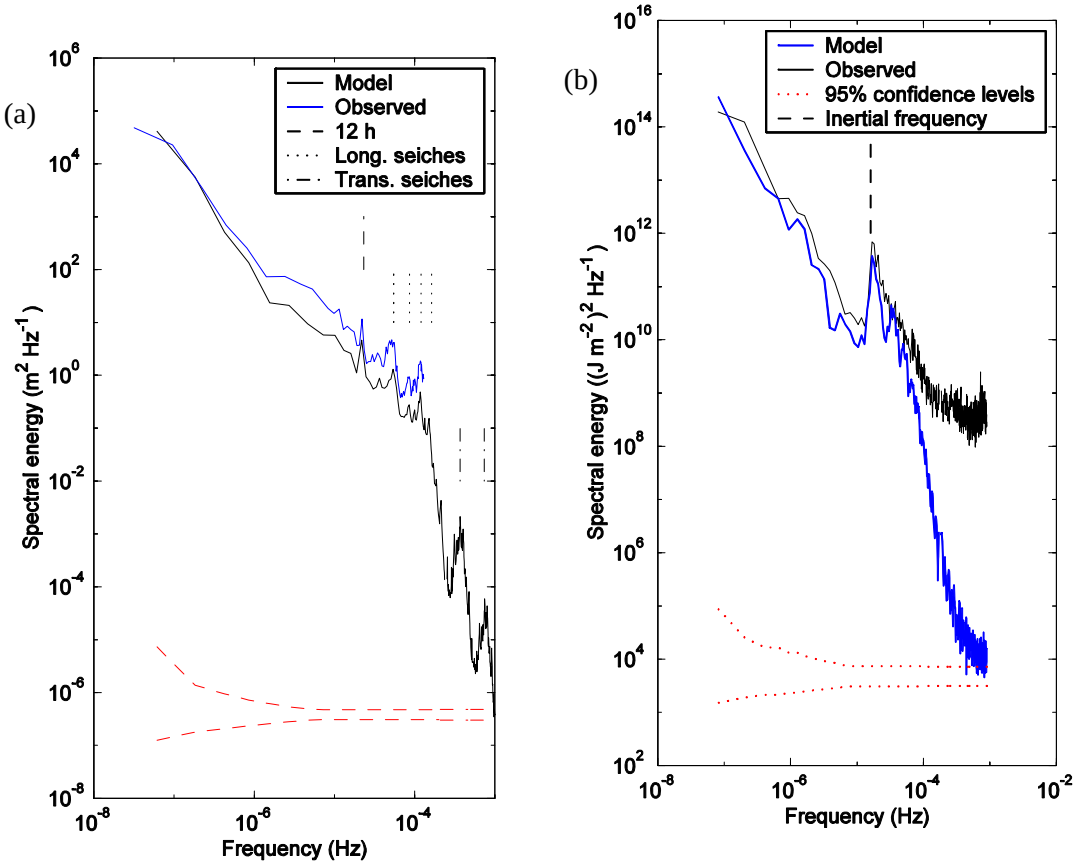

Figure 3: (a) Spectra modelled and observed water levels at station 1263 and Kingston, respectively, from Figure 2. (b) Spectra of modelled and observed vertically integrated potential energy at station 1266 (from Figure 4). The spectra were smoothed in the frequency domain to improve statistical confidence, with the 95% confidence level indicated by the red dotted lines.

others in the Great Lakes and is argued to be a result of finite-amplitude nonlinear effects on the fundamental mode (Mortimer 2006) or higher-mode Poincaré waves (Schwab 1977). Comparison to the observations by (Csanady 1973) suggest that these frequencies correspond to horizontal mode one (H1) and mode three (H3) Poincaré with wavelengths of ~120 km and ~40 km, respectively, running across the ~60 km lake width from Oshawa, NY, to Olcott, NY. From the dispersion relation for Poincaré waves (e.g. Royer et al. 1986) with a phase speed of 50 cm s^{-1}, we compute wavelengths of ~90 km and ~20 km for the transverse H1 and H3 Poincaré modes across the ~45 km lake width at station 1266.

Although the H3 mode is shown observationally to be the dominant Poincaré response through the wider portion of the lake (Csanady 1973), the H1 mode dominates as the lake width tapers towards the western shore. We speculate that this is a response of the wave frequency and wavelength adjusting according to the dispersion relation such that an integer number of odd modes occur across the variable lake width.

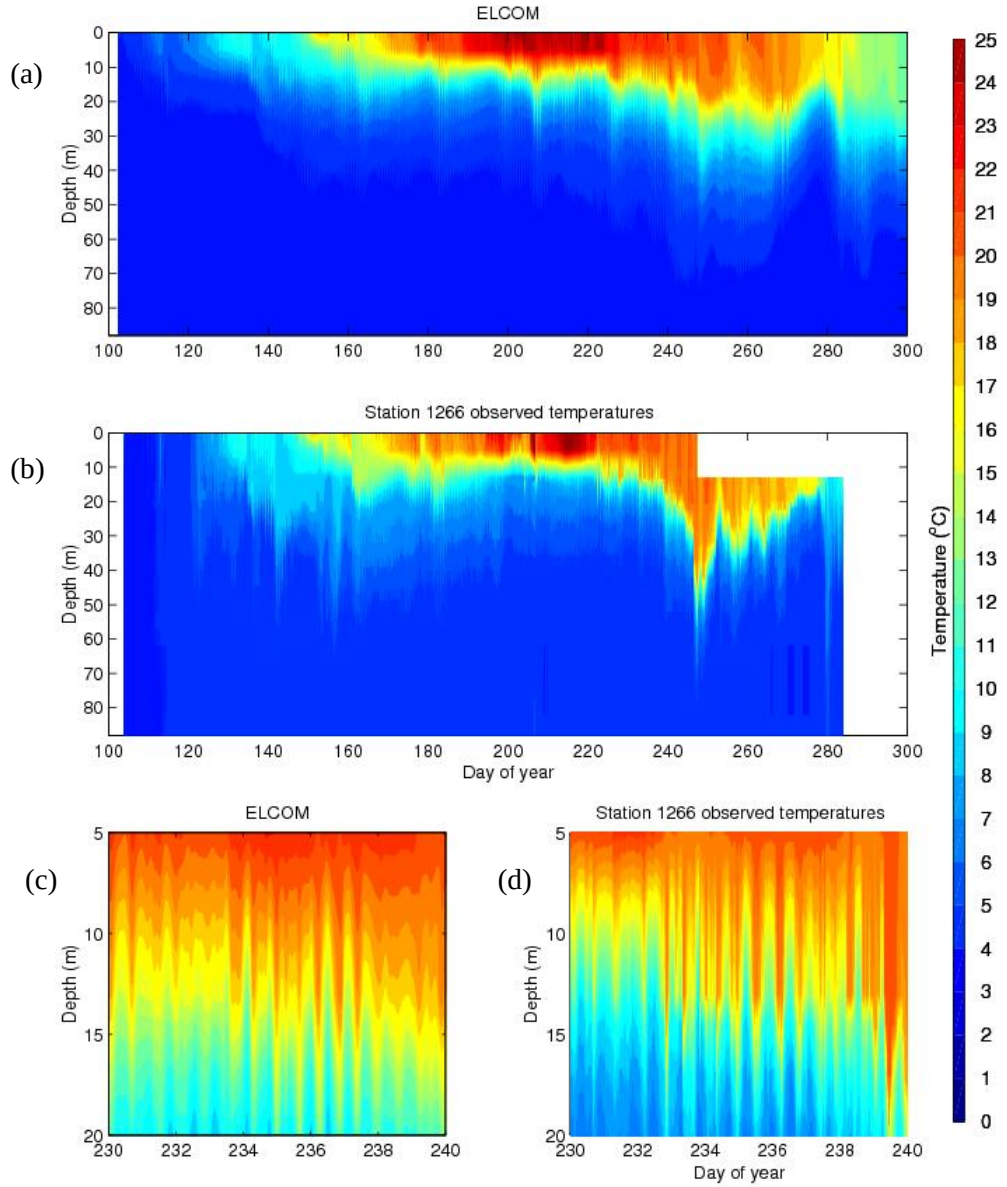

Figure 4: Modelled (a) and observed (b) temperature contours at station 1266. Detail showing modelled (c) and observed (d) Poincaré wave oscillation.

Further analysis of the numerical results is required to fully understand the dynamic modal structure of the Poincaré waves (Hodges et al. 2000). The vertical modal structure has also not yet been investigated (e.g. Royer et al. 1986).

3.3 *Currents*

Modelled currents were compared to observed currents at station 1266 (Fig. 5). The observations were collected at 1 hr intervals using an RDI Workhorse ADCP with 2 m vertical bins. The most notable feature in the east-west (longshore) current observations results from a strong wind event on day 245 (Figs. 5a). As a response to this event, epilimnetic currents oscillate east-west with a magnitude of ~20 cm s^{-1} and a period of ~10 d. These oscillations are primarily barotropic; however, the strong eastward velocity on day 248 has a slight baroclinic component and strong baroclinicity is shown in Fig. 4b near day 245.

Field observations (Csanady. 1976; Rao & Schwab. 2007) have shown similar cyclonic coastal jets associated with barotropic topographic waves (~1 cm amplitude) and baroclinic

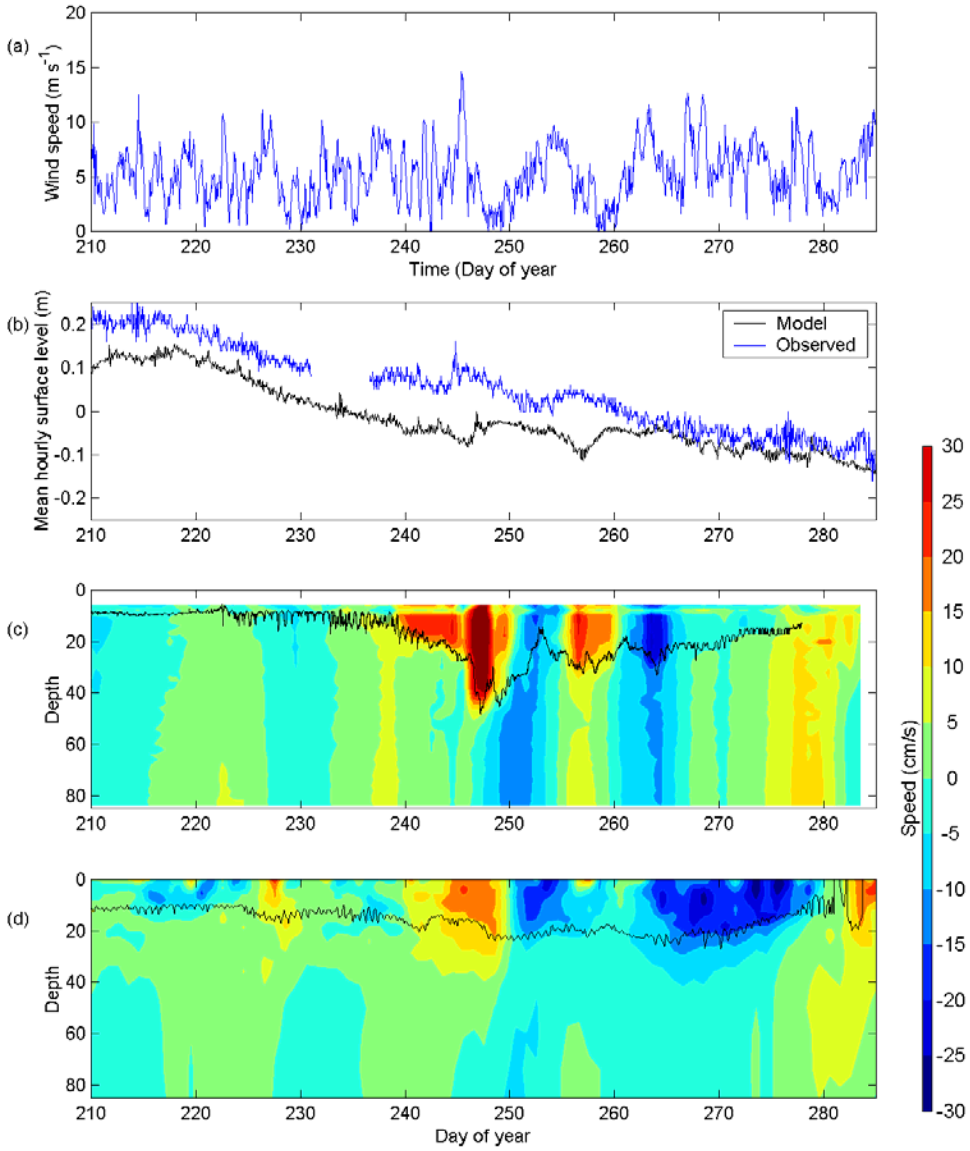

Figure 5: (a) Timeseries of observed hourly wind speed at station 403, measured 3.3 m above the lake surface. (b) Timeseries of observed and modeled hourly water levels at Port Welland and station 1266, respectively. Contours of observed (c) and modelled (d) daily east-west velocity profiles at station 1266. Currents moving east are positive. The black line in panels c and d denotes the 16°C contour from Fig. 4.

Kelvin waves. These waves are difficult to distinguish as they both have phase speeds ~50 cm s^{-1}, current velocities ~20 cm s^{-1} and periods between 10 to 12 days. During fall, weaker stratification leads to a slowing down of the Kelvin wave and a ~1 d phase shift between the waves (Csanady 1976). Comparison of Figs. 5b-d demonstrates that the shallower lower velocity pulse of observed eastward velocity near day 242 (Fig. 5c) is a barotropic topographic wave response resulting from the increased observed water level at this time (Fig. 5b), whereas the deeper eastward observed velocity pulse near day 248 is due to a baroclinic Kelvin wave (Fig. 5c). The composition of these modes in the oscillatory response at later times remains unknown; yet could be investigated through baroclinic and barotropic sensitivity runs.

Figures 5b and 5d show that ELCOM is capturing the free surface elevation and thermocline depression associated with the topographic and Kelvin waves, respectively. However, the modelled surface wave is delayed relative to observed, causing both the baroclinic and barotropic waves to be temporally synchronized within the model domain. Errors in propagation speeds and phasing may be a result of using limited meteorological forcing (Laval et al. 2003). Phase errors are also a result of the motions being under-resolved with the 2 km horizontal grid spacing (Schwab & Beletsky 1998). The Kelvin wave has a characteristic radial length scale of R ~5 km (i.e. the Rossby radius), which is only slightly larger than the 2 km grid resolution and the topographic wave. An $R/5$ or ~1 km grid is required (Schwab & Beletsky 1998). Moreover, the topographic wave has a length scale ~400 km, but significant velocities are confined to a nearshore band ~10 km in width (Csanady 1976).

4 CONCLUSIONS

The hydrodynamic ELCOM model has been shown to be capable of reproducing surface seiches, seasonal stratification and internal Poincaré waves in Lake Ontario using a 2 km horizontal grid. Flow adjustment was required to achieve a water balance. Topographic and internal Kelvin waves are simulated, but are under-resolved. We expect that these motions can be captured with a 1 km horizontal grid.

REFERENCES

Boegman L, Loewen MR, Hamblin PF, Culver DA. 2001. Application of a two-dimensional hydrodynamic reservoir model to Lake Erie. *Can. J. Fish. Aquat. Sci.* 58 : 858-69

Csanady GT. 1976. Topographic waves in Lake Ontario. *J. Phys. Oceanogr*. 6 : 93-103

Csanady GT. 1973. Transverse internal seiches in large oblong lakes and marginal seas. *J. Phys. Oceanogr*. 3 : 439-47

Denison NF. 1908. Lake undulations. *J. Roy. Astron. Soc. Can*. 251

Hamblin PF. 1987. Meterological forcing and water level fluctuations on Lake Erie. *J. Great Lakes Res*. 13 : 436-53

Hamblin PF. 1982. On the free surface oscillations of Lake Ontario. *Limnol. Oceanogr*. 27 : 1039-49

Hodges BR, Imberger J, Saggio A, Winters KB. 2000. Modeling basin-scale internal waves in a stratified lake. *Limnol. Oceanogr*. 45 : 1603-20

Laval B, Imberger J, Hodges BR, Stocker R. 2003. Modeling circulation in lakes: Spatial and temporal variations. *Limnol. Oceanogr*. 48 : 983-94

León LF, Imberger J, Smith REH, Hecky RE, Lam DC, Schertzer WM. 2005. Modeling as a tool for nutrient management in Lake Erie: A hydrodynamics study. *J. Great Lakes Res.* 31(Suppl. 2) : 309-18

Mortimer CH. 2006. Inertial oscillations and related internal beat pulsations and surges in lakes Michigan and Ontario. *Limnol. Oceanogr*. 51 : 1941-55

Prakash S, Atkinson JF, Green ML. 2007. A semi-lagrangian study of circulation and transport in Lake Ontario. *J. Great Lakes Res*. 33 : 774-90

Rao YR, Schwab DJ. 2007. Transport and mixing between the coastal and offshore waters in the Great Lakes: A review. *J. Great Lakes Res*. 33 : 202-18

Royer L, Hamblin PF, Boyce FM. 1986. Analysis of continuous vertical current profiles in Lake Erie. *Atmos. Ocean.* 24 : 73-89

Schwab DJ. 1977. Internal free oscillations in Lake Ontario. *Limnol. Oceanogr*. 22 : 700-8

Schwab DJ, Bedford KW. 1994. Initial implementation of the great lakes forecasting system: A real-time system for predicting lake circulation and thermal structure. *Water Poll. Res. J. Can*. 203-20

Schwab DJ, Beletsky D. 1998. Propagation of Kelvin waves along irregular coastlines in finite-difference models. *Adv. Water Res*. 22 : 239-45